Video Article

Synthesis of Poly(*N*-isopropylacrylamide) Janus Microhydrogels for Anisotropic Thermo-responsiveness and Organophilic/Hydrophilic Loading Capability

Kyoung Duck Seo[1], Andrew Choi[1], Junsang Doh[1,2], Dong Sung Kim[1]

[1]Department of Mechanical Engineering, Pohang University of Science and Technology (POSTECH)

[2]School of Interdisciplinary Bioscience and Bioengineering (I-Bio), Pohang University of Science and Technology (POSTECH)

Correspondence to: Dong Sung Kim at smkds@postech.ac.kr

URL: http://www.jove.com/video/52813
DOI: doi:10.3791/52813

Keywords: Chemistry, Issue 108, Janus particle, hydrogel, microfluidics, poly(*N*-isopropylacrylamide), phase separation of supersaturated *N*-isopropylacrylamide, anisotropic thermo-responsiveness, organophilic/hydrophilic loading capability

Date Published: 2/27/2016

Citation: Seo, K.D., Choi, A., Doh, J., Kim, D.S. Synthesis of Poly(*N*-isopropylacrylamide) Janus Microhydrogels for Anisotropic Thermo-responsiveness and Organophilic/Hydrophilic Loading Capability. *J. Vis. Exp.* (108), e52813, doi:10.3791/52813 (2016).

Abstract

Janus microparticles are compartmentalized particles with differing molecular structures and/or functionality on each of their two sides. Because of this unique property, Janus microparticles have been recognized as a new class of materials, thereby attracting a great deal of attention from various research fields. The versatility of these microparticles has been exemplified through their uses as building blocks for self-assembly, electrically responsive actuators, emulsifiers for painting and cosmetics, and carriers for drug delivery. This study introduces a detailed protocol that explicitly describes a synthetic method for designing novel Janus microhydrogels composed of a single base material, poly(*N*-isopropylacrylamide) (PNIPAAm). Janus microdroplets are firstly generated *via* a hydrodynamic focusing microfluidic device (HFMD) based on the separation of a supersaturated aqueous NIPAAm monomer solution and subsequently polymerized through exposure to UV irradiation. The resulting Janus microhydrogels were found to be entirely composed of the same base material, featured an easily identifiable compartmentalized morphology, and exhibited anisotropic thermo-responsiveness and organophilic/hydrophilic loading capability. We believe that the proposed method introduces a novel hydrogel platform with the potential for advanced synthesis of multi-functional Janus microhydrogels.

Video Link

The video component of this article can be found at http://www.jove.com/video/52813/

Introduction

Hydrogels are a network of hydrophilic polymer chains.[1] An increasing amount of research in the field of hydrogels has promoted significant advances and revealed their similarity to biological tissues; the properties of hydrogels allow the uptake of large amounts of water while maintaining their structure. Environmentally responsive hydrogels have also been studied extensively because of their ability to swell or shrink reversibly in response to external stimuli.[2] Several triggers, including temperature,[3-5] pH,[6,7] light,[8,9] electric fields,[10,11] and specific molecules, such as glucose,[12,13] have been suggested to control the geometric shape of hydrogels. Among the many environmentally responsive hydrogels currently available, poly(*N*-isopropylacrylamide) (PNIPAAm), a well-known thermo-responsive hydrogel, exhibits volume shrinkage above a low critical solution temperature (LCST) of 32 °C.[14] A recent study by Sasaki *et al.*[15] reported the intriguing liquid-liquid phase separation of supersaturated NIPAAm, which is the monomer of PNIPAAm. According to this report, supersaturated NIPAAm was dissolved with a 10-fold molar excess of H_2O, and soon after, the solution separated into two liquid phases when allows to stand at a temperature above 25 °C; by contrast, dilute NIPAAm was dissolved homogeneously under the same conditions.

Microparticles made of environmentally responsive hydrogels are fascinating candidates for application in drug delivery,[16,17] catalysis,[18] sensing,[19,20] and photonics.[21] Traditional synthetic methods including emulsion polymerization, are used to produce hydrogel microparticles with polydispersity.[22,23] However, certain applications require microparticles with a narrow size distribution, for example, to stabilize the pharmacokinetics of drug delivery.[24] Irregularly shaped or polydisperse embolic microparticles aggregate proximally into clusters, leading to chronic inflammatory responses in embolic particles for cancer therapeutic treatment.[25,26]

The microfluidic approach is at the forefront of research as a means of fabricating micro-sized particles with narrow size distributions and complex shapes.[27-31] The advantages of fabricating microparticles in the microfluidic device are predicated by the small characteristic length of the microfluidic device, which results in a low Reynolds number. In contrast to traditional bulk emulsification where drops are formed in parallel, microdroplets produced in microfluidic devices are generated in series and subsequently polymerized into microparticles upon exposure to UV irradiation. The fundamental principle of droplet formation using a microfluidic device is balance between the interfacial tension and the shear force of the sheath fluid acting on the core fluid.

Despite the obvious advantages of microfluidic fabrication of droplets/particles, Janus droplets/particles consisting of the same base material are rarely reported because the internal morphology of these droplets/particles is generally disturbed by the diffusion and perturbation of the core fluids. To circumvent this intrinsic limitation, two groups recently reported the preparation of the Janus microparticles by employing heat-induced phase separation of colloidal nanoparticles and UV-directed phase separation.[32,33]

To this end, we report a microfluidic approach to synthesize Janus microhydrogels entirely composed of a single base material and obtain a product with clearly compartmentalized morphology. Our approach is based on the primary concept of liquid-liquid phase separation of supersaturated NIPAAm monomer. The resulting Janus microhydrogels were found to possess unique properties including anisotropic thermo-responsiveness and organophilic/hydrophilic loading capability.

Protocol

1. Fabrication of a Master Mold for the Hydrodynamic Focusing Microfluidic Device (HFMD) through Photolithography

1. Design a photomask for the HFMD (**Figure 1a**) using computer-assisted design (CAD) software according to the manufacturer's protocol.
2. Rinse a 4' silicon wafer with acetone, isopropyl alcohol (IPA), and deionized (DI) water to remove organic and inorganic dust from the wafer.
3. Clean the silicon wafer with O_2 plasma at 100 W of power for 5 min to increase the bonding strength between the wafer and SU-8.
4. Spin-coat 4 ml of the negative photoresist, SU-8 2150, onto the wafer at 3,000 rpm for 30 sec to achieve a thickness of 150 µm (**b1** in **Figure 1b**).
5. Place the SU-8 coated wafer on a hotplate for 5 min at 65 °C, set the temperature to 95 °C, and then leave the wafer on the hotplate for 30 min to soft bake.
6. Place the designed photomask over the wafer and expose to UV light (260 mJ cm^{-2}, 26 sec for 10 mW cm^{-2}) in a mask aligner (b2 in **Figure 1b**).
7. Perform post-exposure baking on a hotplate (65 °C for 5 min and then 95 °C for 12 min).
8. Develop the wafer by immersion in a SU-8 developer bath for 10 min, and then transfer it into fresh developer for 5 sec to obtain a clean surface.
9. Rinse the wafer for 20 sec with DI water and dry it for 10 sec with N_2 gas (b3 in **Figure 1b**). Use the fabricated wafer as a master mold for polydimethylsiloxane (PDMS) casting in Section 2.

2. Fabrication of the HFMD through PDMS Casting

1. Use the patterned wafer obtained in Section 1 as the master mold for PDMS casting.
2. Mix the PDMS pre-polymer and a curing agent homogeneously at a weight ratio of 10:1; for example, use 1 g of curing agent for 10 g of PDMS pre-polymer.
3. Pour the PDMS pre-polymer into the master mold and degas it for 1 hr in a vacuum chamber (b4 in **Figure 1b**).
4. Place the master mold with the PDMS pre-polymer into an oven at 65 °C for 3 hr.
5. Cut the cured PDMS into the size of a single chip using a sharp scalpel. Carefully peel off the cured PDMS replica from the master mold by hand.
6. Repeat Steps 2.2 to 2.5 to obtain an identical PDMS replica.
7. Punch inlet and outlet holes into one of the replicas using a hole-puncher with a slightly smaller diameter than the outer diameter of the connecting tubing.
8. Apply air plasma treatment to the bonding area of each replica using a corona treater.[34]
   Caution**:** Use the corona treater in an area with good ventilation to avoid ozone buildup.
9. Drop 5 µl of methanol onto the air plasma-treated areas. Finely align two identical PDMS replicas to fabricate the HFMD by hand manipulation, and check alignment *via* a microscope (b5 in **Figure 1b**).
   Note: The air plasma-treated PDMS replicas are fairly sticky and difficult to manipulate. Thus, 5 µl of methanol is added to the air plasma-treated surface to function as a lubricant.
10. Place the HFMD in an oven set to 65 °C overnight to strengthen the bond between two PDMS replicas (b6 in **Figure 1b**). Bond two identical PDMS replicas to increase the height of the microchannel of the HFMD and avoid clogging of microdroplets in the microfluidic channel during operation.

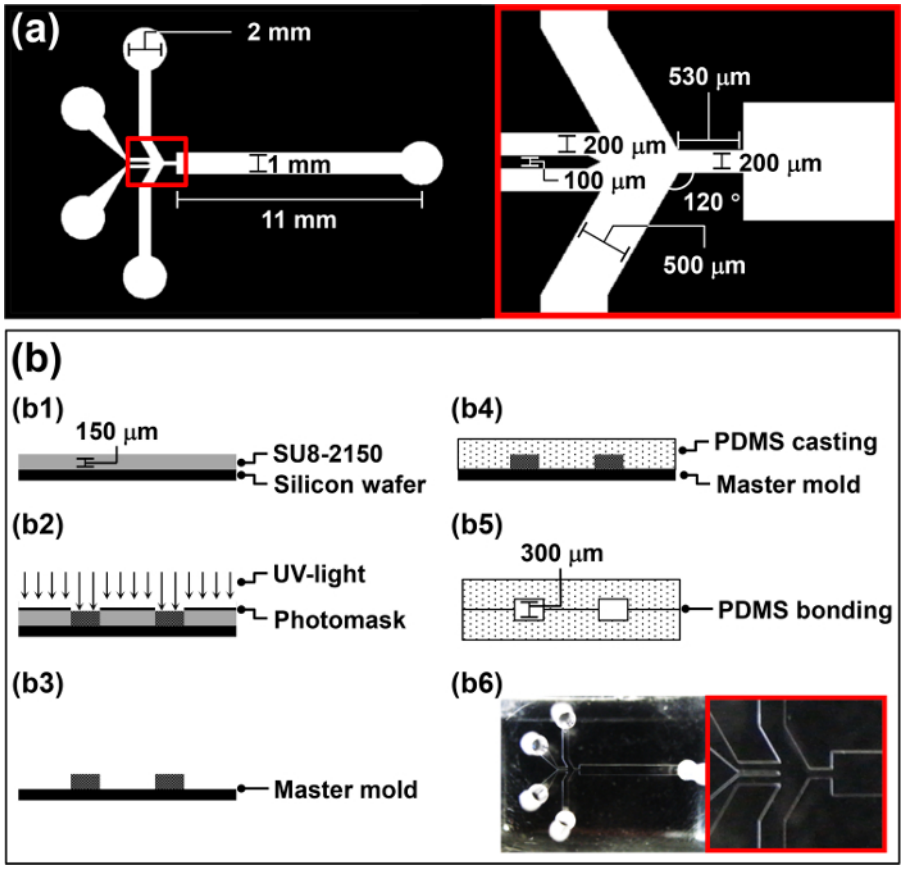

Figure 1: Overview of the HFMD Fabrication Procedure. (**a**) Design parameters of the photomask for the HFMD. (**b**) Illustration of the fabrication procedure for the HFMD. Please click here to view a larger version of this figure.

3. Preparation of NIPAAm-rich (N-rich) and NIPAAm-poor (N-poor) Phases by Phase Separation of Supersaturated NIPAAm

1. Dissolve NIPAAm monomer in DI water at a w/w ratio of 1:1 using a vortex mixer; for example, dissolve 10 g of NIPAAm in 10 ml of DI water (first image of **Figure 2a**).
   Note: Once the NIPAAm monomer is fully dissolved at room temperature, the solution appears turbid (second image of **Figure 2a**). This phenomenon is the first cue that solubility-induced phase separation of the supersaturated NIPAAm monomer has successfully occurred.
2. Allow the monomer solution to rest in a vertical position at room temperature for at least 15 min. The top phase is the N-rich phase, and the denser bottom phase is the N-poor phase (third image of **Figure 2a**). The densities of the N-rich and N-poor phases are 0.93 ± 0.01 and 0.99 ± 0.01 g cm^{-3}, respectively.[15]
3. When the interface separating the two phases becomes clear, carefully extract 2 ml of monomer solution from the N-rich and N-poor phases without disturbing this interface by using a pipette.
4. Add 4 mg of *N*,*N*'-methylenebisacrylamide (MBAAm) as a crosslinker and 4 mg of 4-(2-hydroxyethoxy)phenyl-(2-hydroxy-2-propyl)ketone as a photoinitiator to the extracted N-rich and N-poor monomer solutions to prepare core fluids 1 and 2 for the low crosslinker concentration (2 mg ml^{-1}) sample (b1 and b2 in **Figure 2b**).
5. Repeat previous Step 3.3 and add 80 mg of MBAAm and 4 mg of 4-(2-hydroxyethoxy)phenyl-(2-hydroxy-2-propyl)ketone into each of extracted N-rich and N-poor monomer solution to prepare core fluids 1 and 2 for the high crosslinker concentration (40 mg ml^{-1}) sample (b3 and b4 in **Figure 2b**).
6. Dissolve 10 wt% of oil surfactant into mineral oil to prepare the sheath fluid (b5 in **Figure 2b**).

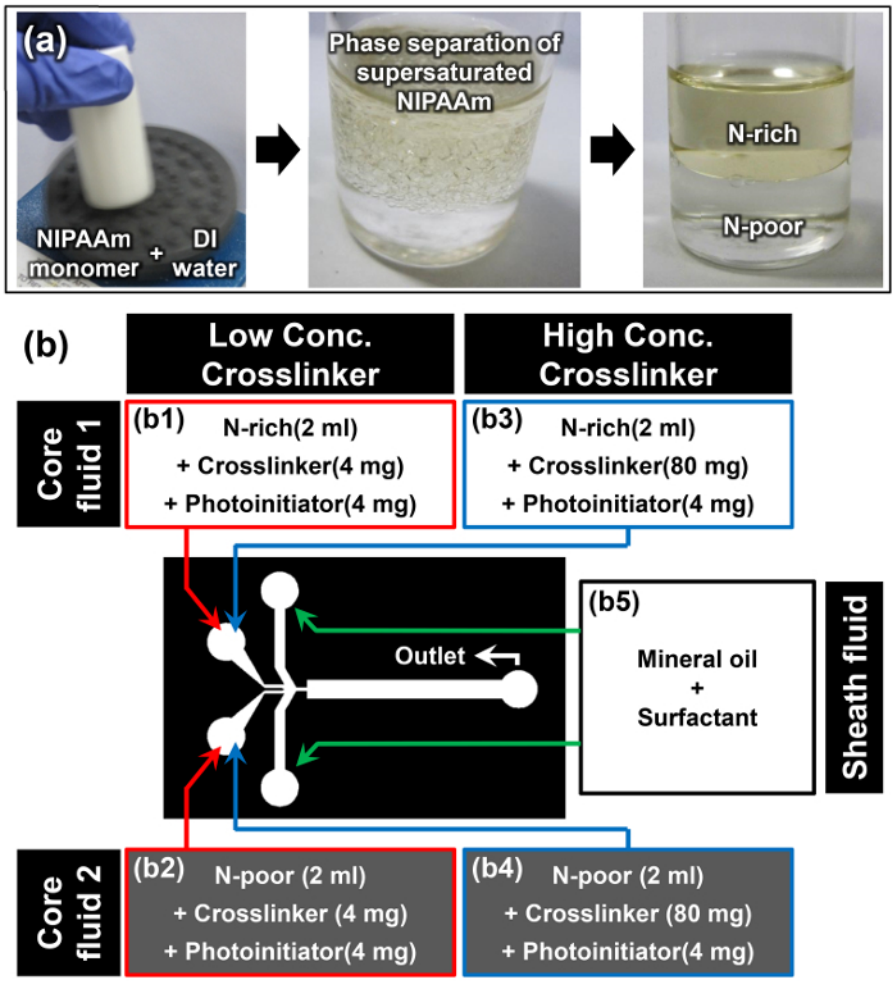

Figure 2: Material Preparation for Janus Microhydrogel Synthesis. (**a**) Preparation of N-rich and N-poor monomer solutions through phase separation of supersaturated NIPAAm. (**b**) Details of the materials and experimental setup used in the protocol. Please click here to view a larger version of this figure.

4. Synthesis of Janus Microhydrogels Using the HFMD

1. Load 2 ml of core fluids 1 and 2 (b1, b2 or b3, b4 in Fi**gure 2b**) and the sheath fluid (b5 in **Figure 2b**) into three separate 3 ml syringes.
2. Mount the syringes into the syringe pumps and connect each syringe to the appropriate fluid inlet of the HFMD using tubing (**Figure (b**). Use tubing to connect the fluid outlet of the HFMD to a collection reservoir.
3. Set the syringe pumps and infuse core fluids 1 and 2 and sheath fluid at flow rates of 2, 2, and 10 µl min^{-1}, respectively.
4. (Optional) Tune the flow rate of core fluids 1 and 2 to adjust the relative volume ratios of each side of the Janus microdroplet.
5. Position the UV light source perpendicularly about 1 cm away from the collection reservoir. Switch on the UV light source and visually monitor the continuous production of Janus microhydrogels.
   Caution**:** Use UV protective-goggles when monitoring microhydrogel production.
6. Collect the fabricated Janus microhydrogels into a conical tube and wash them using IPA. Then, centrifuge the conical tube (780 g for 5 min) to settle the microhydrogels.
7. Repeat Step 4.6 several times to remove the mineral oil surrounding the Janus microhydrogels completely.
8. Repeat Step 4.6 but use DI water with a water surfactant of 0.005% (v/v) instead of IPA to remove the leftover IPA around the Janus microhydrogels.
9. Store completely washed Janus microhydrogels in a 10 ml vial containing DI water.

5. Analysis of the Anisotropic Thermo-responsiveness of Janus Microhydrogels

1. Use a pipette to place Janus microhydrogels synthesized from Section 4 into a 24-well plate. Allow the microhydrogels to settle for 15 sec until a monolayer is formed at the bottom surface of the well.
2. Obtain an image of the Janus microhydrogel at 24 °C using an upright optical microscope with a 5X objective lens.
3. Set a thermoelectric module under the well plate and control the voltage of this module to increase the temperature of the solution containing Janus microhydrogels to 32 °C.
4. Obtain an image of the Janus microhydrogel at 32 °C once more by using an upright optical microscope with a 5X objective lens.

5. Repeat Steps 5.2-5.4 24-times, taking care to choose a different Janus microhydrogel for statistical analysis.
6. From the 25 images of different Janus microhydrogels at 24 and 32 °C, measure the radius of the PN-rich and PN-poor parts of the Janus microhydrogels using image analysis software according to the manufacturer's instructions.

Representative Results

Figure 3a presents a schematic of the experimental setup used to synthesize Janus microhydrogels *via* the HFMD. The N-rich and N-poor phases were precisely injected into the HFMD as core fluids 1 and 2 and then merged and broken up into Janus microdroplets at the orifice by the sheath fluid of mineral oil because of the Rayleigh capillary instability. Consequently, Janus microdroplets composed of N-rich and N-poor phases were successfully generated as shown in **Figure 3b**. The diameter of the microdroplets was 190 µm with coefficient of variation (CV) of less than 2%. The clearly compartmentalized internal morphology of the Janus microdroplets was observed since both phases are stably separated. It should be noted that each phase is immiscible in the other and diffusion between the phases is nearly negligible. The volume ratio of the N-rich and N-poor phases inside a microdroplet was controlled by altering the flow rate of each monomer solution through the syringe pump, as shown in **Figure 3c**. The photoinitiator added in the N-rich and N-poor monomer solutions was then triggered by exposure to UV-light, thereby inducing the polymerization of the N-rich and N-poor phases to PN-rich and PN-poor, respectively.

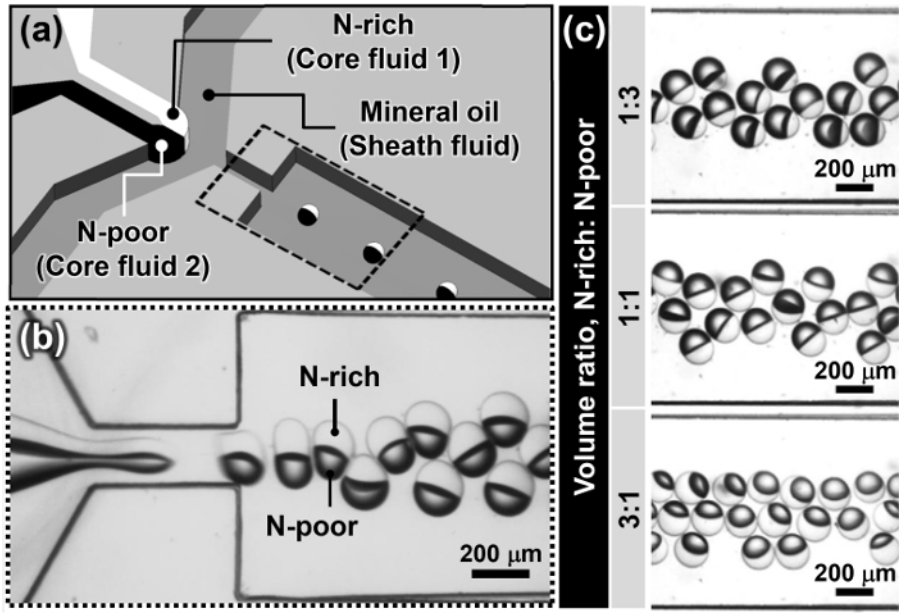

Figure 3: Generation of Janus Microdroplets using the HFMD. (**a**) Schematic diagram of the HFMD for generating Janus microdroplets. (**b**) Optical micrograph of the Janus microdroplets composed of N-rich and N-poor phases. (**c**) Janus microdroplets obtained with different volume ratios of the N-rich and N-poor phases (1:3, 1:1, 3:1). Please click here to view a larger version of this figure.

Figure 4 depicts the anisotropic thermos-responsive behavior of the microhydrogels caused by differences in NIPAAm monomer concentration between the PN-rich and PN-poor parts of the Janus microhydrogel. Janus microhydrogels with different crosslinker concentrations of 2 and 40 mg ml^{-1} were fabricated to examine the effect of crosslinker concentration on the thermo-responsive behavior of the resultant hydrogels. As shown in **Figure 4**, increases in crosslinker concentration resulted in decreases in the reversible volume change of the microhydrogels above and below the LCST.

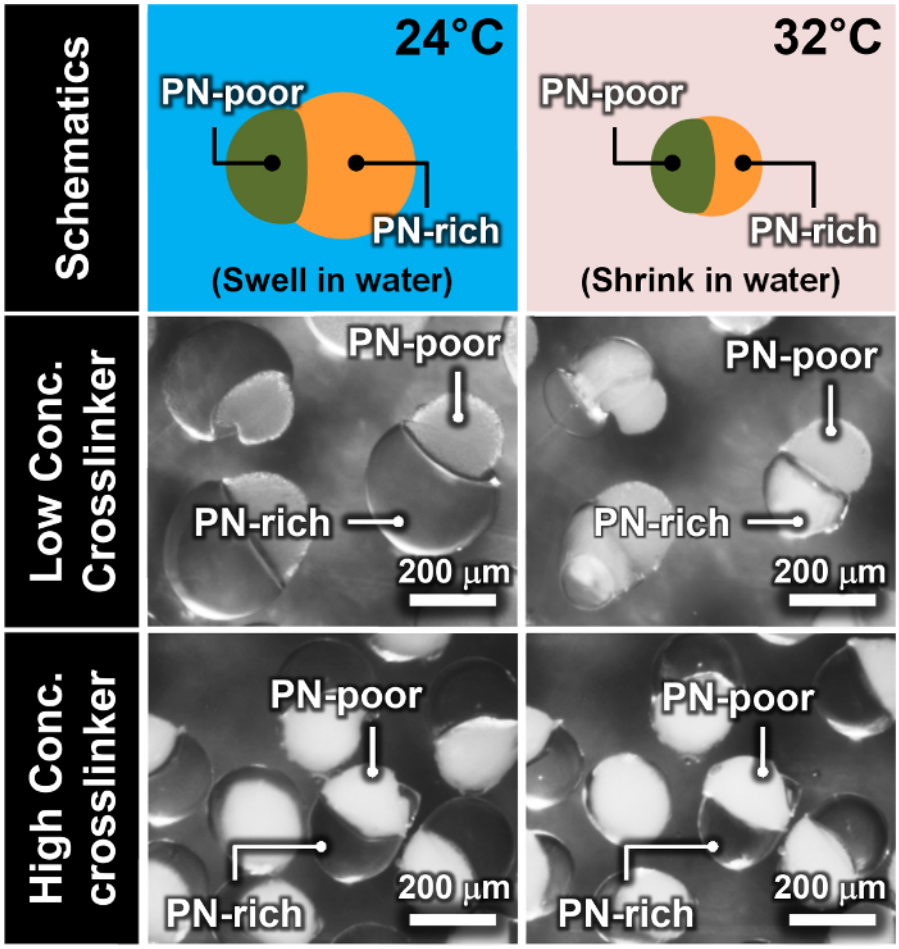

Figure 4: Temperature Response of the Janus Microhydrogels. Anisotropic volume changes in the Janus microhydrogels in response to temperature variation were induced by differences in NIPAAm monomer concentration between the PN-rich and PN-poor parts. Please click here to view a larger version of this figure.

Figure 5a shows schematic diagrams and optical micrographs of the Janus microdroplets/microhydrogels in response to environmental and temperature changes: 24 °C in oil, 24 °C in water, and 32 °C in water. To quantify thermo-responsiveness, we measured the radius of the Janus microdroplets/microhydrogels, as shown in **Figure 5b**. The error bar in **Figure 5b** represents the standard deviation of the measured radius in 25 Janus microhydrogels. The radius of each part of the Janus microhydrogels was determined from the captured images using image analysis software. In the monomer droplet state (a1 in **Figure 5a** and **Figure 5b**), the radius of the N-rich and N-poor phases was nearly identical. A slight difference in radius between the PN-rich and PN-poor parts of the Janus microhydrogels was observed after polymerization (a2 in **Figure 5a** and **Figure b**) due to the lower NIPAAm monomer concentration in the N-poor phase compared with that in the N-rich phase. Both PN-rich and PN-poor parts of the Janus microhydrogels were fully swollen in DI water at room temperature. In the swelling stage, the swelling of the PN-rich part was greater than that of the PN-poor part; consequentially, snow-man shaped Janus microhydrogels were obtained (a3 in **Figure 5a** and **Figure b**). Interestingly, the radius of the microhydrogels after shrinking at 32 °C was similar to the radius of the microdroplets generated in the HFMD (a4 in **Figure 5a** and **Figure 5b**).

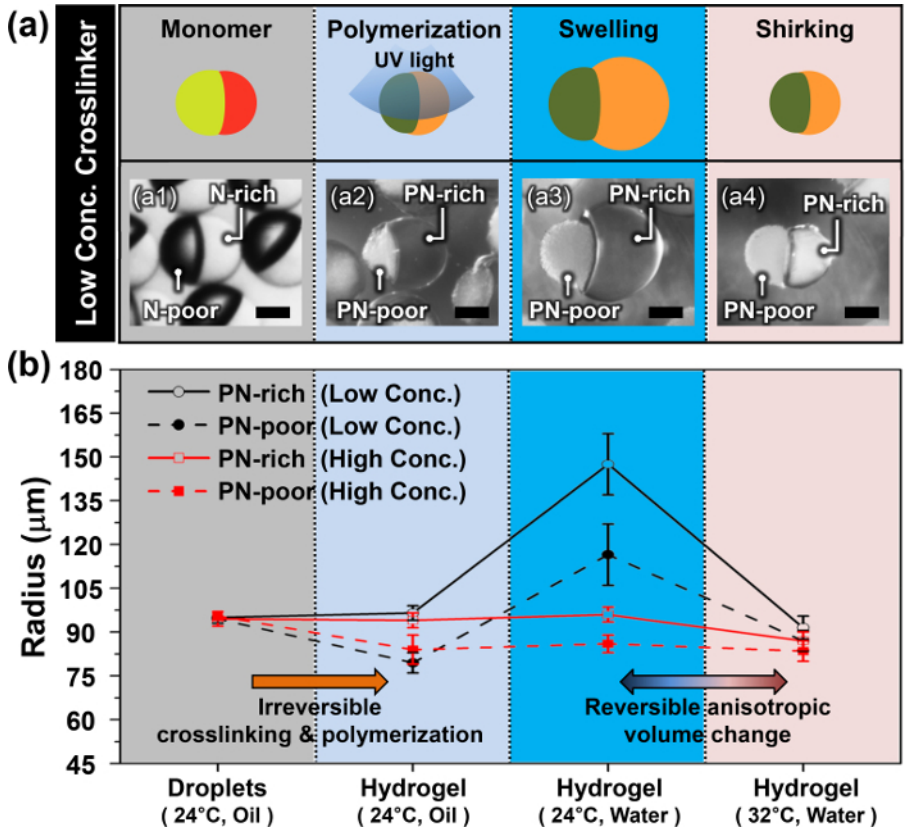

Figure 5: Janus Microhydrogels with Anisotropic Thermo-Responsiveness. (**a**) Schematic diagrams and optical micrographs of Janus microdroplets/microhydrogels (Scale bars are 100 μm). (**b**) Radius change of the Janus microdroplets/microhydrogels in response to environmental and temperature change: 24 °C in oil, 24 °C in water, and 32 °C in water. Please click here to view a larger version of this figure.

Figure 6a shows the dissolution properties of the N-rich and N-poor monomer solutions. Fat-soluble dye (oil red O and oil blue N) and water-soluble dye (yellow and green food dyes) strongly prefer to dissolve into the N-rich and N-poor monomer solutions, respectively. Based on these dissolution characteristics, Janus NIPAAm monomer microdroplets containing fat- and water-soluble dyes without cross-mixing were generated by using the proposed protocol. Oil red O and green food dye were respectively selected as representative organophilic and hydrophilic materials, as shown in **Figure 6b**. After UV polymerization, Janus microhydrogels containing both dyes were successfully synthesized, shown in **Figure 6c.** These results reveal that the Janus microhydrogel could be applied as organophilic/hydrophilic dual material carriers.

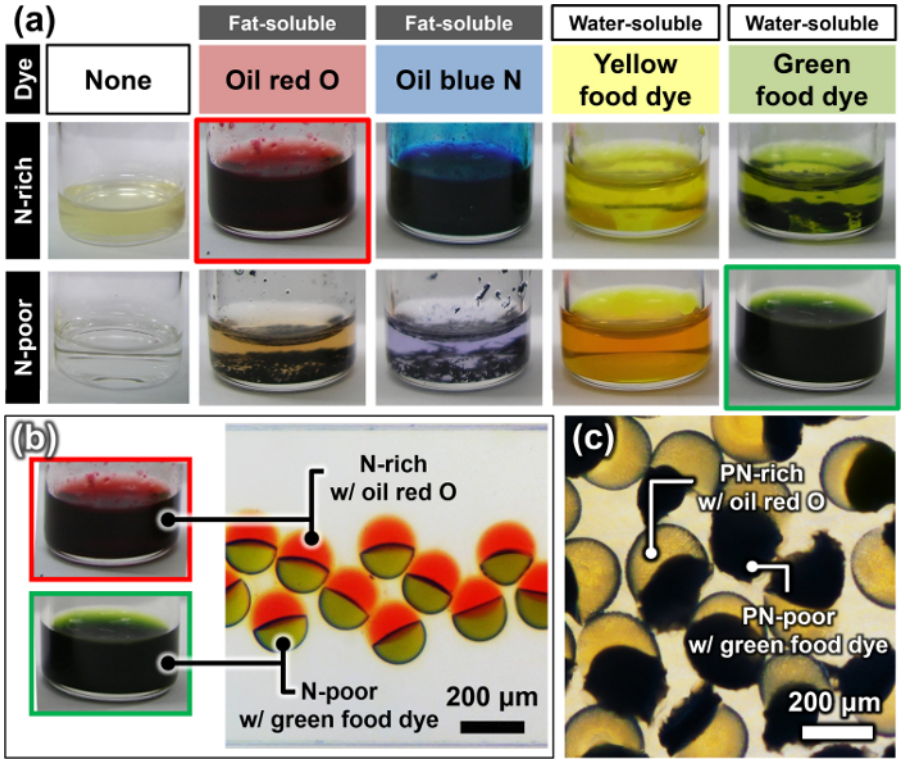

Figure 6: Janus Microhydrogels with Organophilic/Hydrophilic Loading Capability. (**a**) Dissolution properties of N-rich and N-poor monomer solutions. Fat- and water-soluble dyes strongly preferred to dissolve in the N-rich and N-poor monomer solutions, respectively. (**b**) Generation of Janus microdroplets containing fat- and water-soluble dyes without cross-mixing. (**c**) Polymerized Janus microhydrogels containing fat- and water-soluble dyes. Please click here to view a larger version of this figure.

Discussion

Two immiscible base materials are generally used to synthesize the Janus microhydrogels. Until recently, Janus microhydrogels consisting of the same base material were rarely reported and the reported Janus microhydrogels did not have a clear internal morphology due to the disturbance caused by the miscibility of the component materials.[35, 36] In this protocol, we demonstrate a method to synthesize Janus microhydrogels composed entirely of the single base material, PNIPAAm, with a clearly compartmentalized structure.

As a critical step to synthesize the Janus microhydrogels, we introduced the phase separation phenomenon of the supersaturated NIPAAm monomer solution. The N-rich and N-poor phase solutions collected from the phase separation phenomenon are immiscible and the disturbance between the N-rich and N-poor phase is nearly negligible. This immiscibility of the N-rich and N-poor phases in the Janus microdroplets was maintained in the HFMD and the morphology of the Janus microhydrogels was preserved even after polymerization.

We applied the HFMD as a method to synthesize the Janus microhydrogels because the protocol enables the facile production of monodisperse Janus microhydrogels with a rate of 10^5 Janus microhydrogels per hour. The newly designed HFMD in this work was properly fabricated for producing Janus microhydrogels with sizes within the order of a hundred micrometers; future designs of HFMD may be able to produce Janus microhydrogels of a smaller size.

Further study of the Janus microhydrogels revealed two distinct characteristics originating from different NIPAAm concentrations in the N-rich and N-poor phases. First, the Janus microhydrogels composed of different NIPAAm concentrations exhibited anisotropic thermo-responsive behaviors in response to temperature variance. The monomer to crosslinker ratio is well known to directly influence the level of swelling of a hydrogel.[37] The amount of NIPAAm molecules in the N-rich phase is generally much higher than that in the N-poor phase; thus, the monomer to crosslinker ratio in the N-rich phase is greater than that in the N-poor phase when an identical concentration of crosslinker is used for both phases. Consequently, the PN-rich part of the Janus hydrogel undergoes a larger volume change compared with the PN-poor part in response to temperature change. Second, the Janus microhydrogels exhibited organophilic/hydrophilic loading capability without cross-mixing. The fat-soluble dye was well-dissolved in the N-rich monomer solution while the water-soluble dye was well-dissolved in the N-poor monomer solution. The contrasting dissolution properties of the N-rich and N-poor monomer solutions are derived from differences in the availability of free water molecules left over after interacting with NIPAAm molecules in each monomer solution. Because it possesses a comparably higher number of leftover free water molecules than the N-rich monomer solution, the N-poor monomer solution can easily dissolve hydrophilic polar molecules within the water-soluble dye. By contrast, water-soluble dye exhibited poor solubility in the N-rich monomer solution, which can only interact with a few free water molecules. Consequently, the N-rich and N-poor monomer solutions showed opposite results when mixed with fat-soluble dye. The synthesized Janus microhydrogels may be used as organophilic/hydrophilic dual material carriers with a compartmentalized internal morphology without cross-mixing.

Future application

The novel characteristics of Janus microhydrogels can be utilized to develop functional microparticles and achieve multiple-drug encapsulation. We believe that the synthetic protocol for these Janus microhydrogels based on phase separation of the supersaturated NIPAAm introduces a novel material platform with the potential for advanced synthesis of multi-functional Janus microhydrogels.

Disclosures

The authors declare that they have no competing financial interests.

Acknowledgements

This work was supported by the National Research Foundation of Korea (NRF) grant funded by the Korea Government (MSIP (Nos. 2014R1A2A1A01006527 and 2011-0030075).

References

1. Hoffman, A. S. Hydrogels for biomedical applications. *Adv. Drug Delivery Rev.* **54** (1), 3-12 (2002).
2. Qiu, Y., & Park, K. Environment-sensitive hydrogels for drug delivery. *Adv. Drug Delivery Rev.* **53** (3), 321-339 (2001).
3. Hirokawa, Y., & Tanaka, T. Volume phase transition in a nonionic gel. *J. Chem. Phys.* **81** (12), 6379-6380 (1984).
4. Bae, Y. H., Okano, T., Hsu, R., & Kim, S. W. Thermo-sensitive polymers as on-off switches for drug release. *Macromol. Rapid Commun.* **8** (10), 481-485 (1987).
5. Yoshida, R. *et al.* Comb-type grafted hydrogels with rapid deswelling response to temperature changes. *Nature* **374** (6519), 240-242 (1995).
6. Tanaka, T. Collapse of gels and the critical endpoint. *Phys. Rev. Lett.* **40** (12), 820-823 (1978).
7. Tanaka, T. *et al.* Phase transitions in ionic gels. *Phys. Rev. Lett.* **45** (20) 1636-1639 (1980).
8. Zhao, Y. L., & Stoddart, J. F. Azobenzene-based light-responsive hydrogel system. *Langmuir*. **25** (15), 8442-8446 (2009).
9. Alvarez-Lorenzo, C., Bromberg, L., & Concheiro, A. Light-sensitive intelligent drug delivery systems. *Photochem. Photobiol.* **85** (4), 848-860 (2009).
10. Tanaka, T., Nishio, I., Sun, S. T., & Ueno-Nishio, S. Collapse of gels in an electric field. *Science*. **218** (4571), 467-469 (1982).
11. Kwon, I. C., Bae, Y. H., & Kim, S. W. Electrically credible polymer gel for controlled release of drugs. *Nature*. **354** (6351), 291-293 (1991).
12. Obaidat, A. A., & Park, K. Characterization of protein release through glucose-sensitive hydrogel membranes. *Biomaterials*. **18** (11), 801-806 (1997).
13. Kataoka, K., Miyazaki, H., Bunya, M., Okano, T., & Sakurai, Y. Totally synthetic polymer gels responding to external glucose concentration: their preparation and application to on-off regulation of insulin release. *J. Am. Chem. Soc.* **120** (48), 12694-12695 (1998).
14. Heskins, M., & Guillet, J. E. Solution properties of poly(*N*-isopropylacrylamide). *J. Macromol. Sci. Part A Pure Appl. Chem.* **2** (8), 1441-1455 (1968).
15. Sasaki, S., Okabe, S., & Miyahara, Y. Thermodynamic properties of *N*-isopropylacrylamide in water: solubility transition, phase separation of supersaturated solution, and glass formation. *J. Phys. Chem. B*. **114** (46), 14995-15002 (2010).
16. Bromberg, L., & Alakhov, V. Effects of polyether-modified poly(acrylic acid) microgels on doxorubicin transport in human intestinal epithelial Caco-2 cell layers. *J. Controlled Release*. **88** (1), 11-22 (2003).
17. Coughlan, D. C., Quilty, F. P., & Corrigan, O. I. Effect of drug physicochemical properties on swelling/deswelling kinetics and pulsatile drug release from thermoresponsive poly(*N*-isopropylacrylamide) hydrogels. *J. Controll. Release*. **98** (1), 97-114 (2004).
18. Bergbreiter, D. E., Case, B. L., Liu, Y. S., & Caraway, J. W. Poly(*N*-isopropylacrylamide) soluble polymer supports in catalysis and synthesis. *Macromolecules*. **31** (18), 6053-6062 (1998).
19. Lapeyre, V., Gosse, I., Chevreux, S., & Ravaine, V. Monodispersed glucose-responsive microgels operating at physiological salinity. *Biomacromolecules*. **7** (12), 3356-3363 (2006).
20. Hoare, T., & Pelton, R. Engineering glucose swelling responses in poly(*N*-isopropylacrylamide)-based microgels. *Macromolecules*. **40** (3), 670-678 (2007).
21. Xu, S., Zhang, J., Paquet, C., Lin, Y., & Kumacheva, E. From hybrid microgels to photonic crystals. *Adv. Funct. Mater.* **13** (6), 468-472 (2003).
22. Clarke, J., & Vincent, B. Stability of non-aqueous microgel dispersions in the presence of free polymer. *J. Chem. Soc., Faraday Trans. 1.* **77** (8), 1831-1843 (1981).
23. Mears, S. J., Deng, Y., Cosgrove, T., & Pelton, R. Structure of sodium dodecyl sulfate bound to a poly (NIPAM) microgel particle. *Langmuir*. **13** (7), 1901-1906 (1997).
24. Shah, R. K., Kim, J. W., Agresti, J. J., Weitz, D. A., & Chu, L. Y. Fabrication of monodisperse thermosensitive microgels and gel capsules in microfluidic devices. *Soft Matter*. **4** (12), 2303-2309 (2008).
25. Jack, C. R., Forbes, G., Dewanjee, M. K., Brown, M. L., & Earnest, F. Polyvinyl alcohol sponge for embolotherapy: particle size and morphology. *Am. J. Neuroradiol.* **6** (4), 595-597 (1985).
26. Derdeyn, C. P., Moran, C. J., Cross, D. T., Dietrich, H. H., & Dacey, R. G. Polyvinyl alcohol particle size and suspension characteristics. *Am. J. Neuroradiol*. **16** (6), 1335-1343 (1995).
27. Han, K. *et al.* Effect of flow rates on generation of monodisperse clay-poly(*N*-isopropylacrylamide) embolic microspheres using hydrodynamic focusing microfluidic device. *Jpn. J. Appl. Phys.* **50** (6), 06GL12 (2011).
28. Seo, K. D., Doh, J., & Kim, D. S. One-step microfluidic synthesis of Janus microhydrogels with anisotropic thermo-responsive behavior and organophilic/hydrophilic loading capability. *Langmuir*. **29** (49), 15137-15141 (2013).
29. Seo, K. D., & Kim, D. S. Microfluidic synthesis of thermo-responsive poly(*N*-isopropylacrylamide)-poly(ethylene glycol) diacrylate microhydrogels as chemo-embolic microspheres. *J. Micromech. Microeng.* **24** (8), 085001 (2014).
30. Seo, K. D., Kwak, B. K., Kim, D. S., & Sánchez, S. Microfluidic-assisted fabrication of flexible and location traceable organo-motor. *IEEE Trans. Nanobiosci.* **14** (3), 298-304 (2015).
31. Seo, K. D., Kim, D. S., & Sánchez, S. Fabrication and application of complex-shaped microparticles *via* microfluidics. *Lab Chip.* (2015).

32. Shah, R. K., Kim, J. W., & Weitz, D. A. Janus supraparticles by induced phase separation of nanoparticles in droplets. *Adv. Mater.* **21** (19), 1949-1953 (2009).
33. Lone, S. *et al.* Microfluidic synthesis of Janus particles by UV-directed phase separation. *Chem. Commun.* **47** (9), 2634-2636 (2011).
34. Hauber, K., Drier, T., & Beebe, D. PDMS bonding by means of a portable, low-cost corona system. *Lab chip*. **6** (12), 1548-1549 (2006).
35. Nisisako, T., Torii, T., Takahashi, T., & Takizawa, Y. Synthesis of monodisperse bicolored Janus particles with electrical anisotropy using a microfluidic co-flow system. *Adv. Mater.* **18** (9), 1152-1156 (2006).
36. Seiffert, S., Romanowsky, M. B., & Weitz, D. A. Janus microgels produced from functional precursor polymers. *Langmuir*. **26** (18), 14842-14847 (2010).
37. Peppas, N. A., Hilt, J. Z., Khademhosseini, A., & Langer, R. Hydrogels in biology and medicine: from molecular principles to bionanotechnology. *Adv. Mater.* **18** (11), 1345-1360 (2006).

